

Proc. of the International Conference on Mechanochemistry and Mechanical Alloying, Kraków, Poland, June 22–26, 2014

Mechanochemical Preparation and Properties of Nanodimensional Perovskite Materials

Z. CHERKEZOVA-ZHELEVA*, D. PANEVA, I. YORDANOVA, M. SHOPSKA AND H. KOLEV
Institute of Catalysis, Bulgarian Academy of Sciences, “Acad. G. Bonchev” Str., Bld. 11, 1113 Sofia, Bulgaria

The study is focused on the synthesis of LaMO_3 ($M = \text{Co, Fe, Mn}$) perovskite materials using combination of precipitation of precursors and mechanical milling at room temperature. Physicochemical properties of products at each step of preparation were studied by powder X-ray diffraction, Mössbauer spectroscopy, infrared spectroscopy (in the middle and far regions) and X-ray photoelectron measurements. As-prepared perovskite powders are composed of nanoparticles with very fine crystallite size (about 15 nm) in all cases. The materials have also high dispersion, high extent of microstrains and high level of oxygen vacancies which is very important in relevance to their use as heterogeneous catalysts.

DOI: [10.12693/APhysPolA.126.916](https://doi.org/10.12693/APhysPolA.126.916)

PACS: 81.07.-b, 82.80.Ej, 82.80.Pv

1. Introduction

The perovskite oxides have the general formula ABO_3 where A and B denote two different cations. The possibility of synthesizing perovskites by partial substitution of cations in positions A or B gives rise to preparation of compounds with unusual oxidation states in the crystal structure. Nowadays, they are intensively studied due to their physical properties like colossal magnetoresistance, ferroelectricity, superconductivity, etc. [1–5]. Different types of perovskites are used as sensors and catalyst electrodes in fuel cells [1–7]. Study of Fe-, Co- and Mn-lantania-based perovskite oxides is one of the main focuses in this regard. In these materials both the bulk-oxygen pathway and the interfacial oxygen reduction kinetics play an important role. It has been shown that surface processes such as the surface oxygen exchange and oxygen surface diffusion influence the catalytic performance of materials [2–7]. Oxygen vacancies can be formed by charge imbalances induced by doping of the materials. In perovskite-type materials, the creation of oxygen vacancies strongly depends on environment, temperature and the type and loading of the B-site cations. Oxygen vacancy formation in Co, Fe, and Mn perovskite-type materials has been studied and the ease of forming oxygen vacancies has been found to increase in the following order: $\text{Mn} < \text{Fe} < \text{Co}$ [2]. Such catalysts are also cheaper than the noble metal supported ones.

Perovskites can be prepared by a conventional solid-state reaction, which results in low disparity and worse catalytic behavior of materials. To obtain materials of higher dispersion a number of synthesis methods have been developed such as hydrothermal synthesis [3], sol-gel and combustion routes [1, 4–6], microemulsion route [7], etc. On the other hand, mechanochemical synthesis (MCS) is an alternative preparation method, which combines the main concepts of a green chemistry

approach and a proper inexpensive technology very suitable for industrial application [8–12]. Some of the main properties of mechanochemistry are very suitable for synthesis of new and advanced materials, as well as of highly effective catalyst preparation either as a step or as a main stage of preparation. Mechanical activation changes the overall reactivity of solids.

Previous studies show preparation of Co-, Fe- and Mn-La-containing perovskite materials by high-energy grinding of mixture of respective oxide powders [9–12]. In order to improve the synthesis and to increase the materials dispersion there were done different investigations on mechanochemical formation of hydroxide materials and preparation of perovskite after their thermal treatment and washing [12, 13]. The detail study of LaMnO_3 preparation shows the role of water content in starting materials. It influences significantly not only their grinding behavior and mechanochemical reaction rate, but the dispersity of prepared composites, too, i.e. their specific surface area, porosity and particle size [14]. Another approach of preparation of highly dispersed perovskite materials could be a grinding of freshly precipitated initial materials. It is well known that such precursors have a great potential for preparation of good catalysts. This study reports the obtained results on the preparation of LaMO_3 ($M = \text{Co, Fe, Mn}$) perovskite catalytic materials by combination of precipitation and mechanochemical method. Characterization of intermediates and synthesized samples was provided by powder X-ray diffraction (XRD), Mössbauer spectroscopy, infrared spectroscopy (IR) and X-ray photoelectron measurements (XPS).

2. Experimental

2.1. Sample preparation

Studied perovskite materials were prepared by precipitation of respective precursors followed by their mechanochemical activation (MA) with La_2O_3 . The preparation procedure was as follows: aqueous solutions of $\text{Mn}(\text{NO}_3)_3 \cdot 4\text{H}_2\text{O}$ (Alfa Aesar, 99.9%) or $\text{Co}(\text{NO}_3)_3 \cdot$

*corresponding author; e-mail: zzhel@ic.bas.bg

6H₂O (Sigma-Aldrich, 99.99%) and Fe(NO₃)₃ · 9H₂O (Sigma-Aldrich, 99.99%) were precipitated using solution of NaOH (Sigma-Aldrich, pellets, ≥ 97%) added slowly at continuous stirring. After that the obtained precipitates were washed during filtering while the solution pH reached neutral value. The samples were dried 12 h at 60 °C. High energy planetary ball mill PM 100, Retsch, Germany was used for MA. The stoichiometric quantity of La₂O₃ (Alfa Aesar, 99.995%) was added to obtained materials. Then the mixtures were milled for 6 h at rotation speed of 600 rpm. The weight ratio between balls and powder was 12:1.

2.2. Sample characterization

Powder X-ray diffraction (XRD) patterns were collected using a TUR-M62 apparatus (Germany) with Co-K_α radiation. Data interpretation was carried out using the JCPDS database. Average crystallite sizes and microstrains were determined from the Williamson–Hall diagram [15]. The Mössbauer spectra were obtained at room temperature with a spectrometer Wissenschaftliche Elektronik GMBN, Germany working in a constant acceleration mode using ⁵⁷Co/Rh (activity ≈ 50 mCi) source and α-Fe standard. The parameters of hyperfine interaction — isomer shift (IS), quadrupole splitting (QS) and magnetic hyperfine field (*H*_{hf}) as well as the line widths (FWHM) and the relative spectral area (*G*) of the partial components of the spectra were determined. Values of errors are on the order of ±0.01 mm/s for the IS, ±0.02 mm/s for the QS, ±2 T for *H*_{eff}, 0.4 mm/s for FWHM and ±2% for *G*, respectively. IR spectra of the samples were recorded by a Nicolet 6700 FTIR spectrometer (Thermo Electron Corporation, USA) in the middle (400–4000 cm⁻¹) and far (250–600 cm⁻¹) regions using KBr pellets. X-ray photoelectron measurements (XPS) have been carried out on the ESCALAB MkII (VG Scientific) electron spectrometer at a base pressure in the analysis chamber of 5 × 10⁻¹⁰ mbar using Al K_α X-ray source (200 W) with excitation energies of 1486.6 eV. The energy scale has been calibrated by normalizing the C1s line of adsorbed adventitious hydrocarbons to 285.0 eV. The relative concentrations of the different chemical species are determined based on normalization of the peak areas to their photoionization cross-sections, calculated by Scofield [16].

3. Results and discussion

3.1. XRD analysis

XRD patterns of precipitated precursors can be seen in Figs. 1a, 2a, and 3a. They are characteristic for the following phases: ferrihydrite and α-FeOOH (Fig. 1a), Mn₃O₄ (Fig. 2a) or Co(OH)₂ (Fig. 3a), respectively. The presented diffractograms show halo and broad lines of low intensity in first two cases or well crystallized Co(OH)₂ phase in the last case. Mechanochemical milling of obtained precursors with stoichiometric quantity of La₂O₃ leads to preparation of respective perovskite materials

with cubic crystal structure. Figure 1b presents the well-pronounced peaks corresponding to LaFeO₃ (PDF-75-0541). Figure 2b shows the powder X-ray diffraction of LaMnO₃ (PDF-75-0440). However in the diffraction pattern of Co-containing perovskite it can be seen the registration of hydroxide phase in addition to the perovskite material (Fig. 3b). According to the reference data [8] this can be avoided with treatment of initial material.

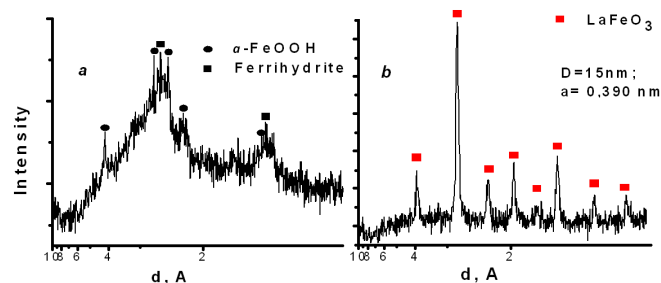


Fig. 1. XRD spectrum of: (a) precipitated iron hydroxide precursor, (b) LaFeO₃ obtained by mechanochemical processing.

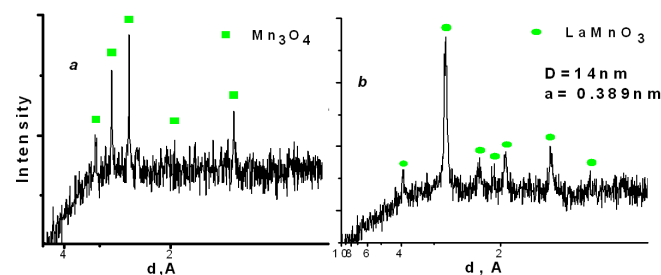


Fig. 2. XRD spectrum of: (a) precipitated Mn₃O₄ precursor, (b) LaMnO₃ obtained by mechanochemical processing of MA precursor.

Mechanoactivation of cobalt containing precursor for 3 h (weight ratio balls/powders = 5:1, 600 rpm) results in decrease of crystallinity degree, as well as in formation of a new phase of Co₃O₄ (Fig. 3c). Prolonged mechanical treatment leads to increase of spinel cobalt oxide phase and decrease of hydroxide phase (not shown), but preparation of such initial material did not lead to better results. Therefore, La₂O₃ was added to as-prepared after 3 h milling cobalt precursor and the mixture was milled for 6 h at 600 rpm. This leads to the formation of single phase LaCoO₃ (PDF-75-0279) (Fig. 3d). Estimation of unit cell parameters and average crystallite sizes was done by evaluation of recorded spectra of obtained monophasic materials (Figs. 1b, 2b, and 3d). Calculated values are presented in the respective figures. The error margins are ±0.005 nm for unit cell parameters and ±3 nm for the average crystallite sizes.

3.2. Mössbauer spectroscopy

The Mössbauer spectra of iron containing samples were registered (Fig. 4). They include superposition of doublet and sextet part. Spectra evaluation was done as an

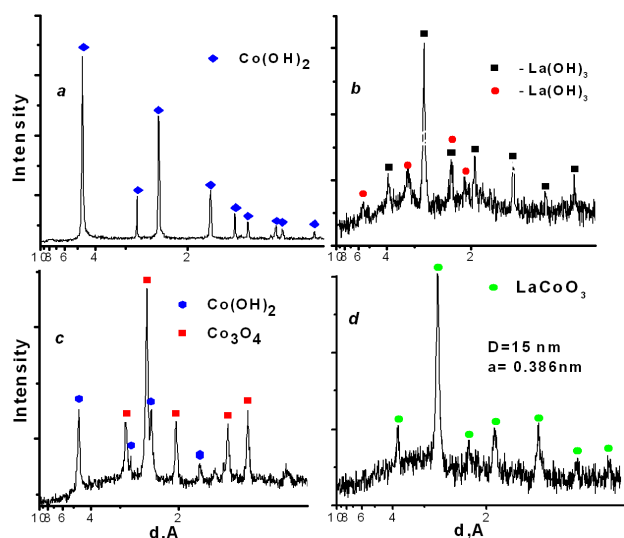


Fig. 3. XRD spectrum of: (a) precipitated cobalt hydroxide precursor, (b) LaCoO_3 obtained by its MA, (c) MA cobalt hydroxide precursor, (d) LaCoO_3 obtained by MA of milled precursor.

optimal fit of component superposition. It can be seen that the spectrum of prepared iron hydroxide precursor (Fig. 4a) includes a paramagnetic doublet (about 86%) and lower quantity of sextet component (about 14%).

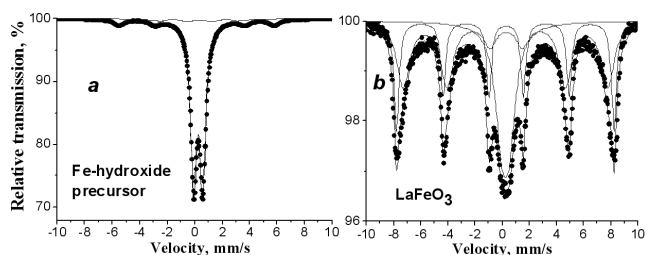


Fig. 4. Mössbauer spectrum of: (a) precipitated iron hydroxide precursor, (b) LaFeO_3 obtained by mechanochemical processing.

The calculated parameter values of these components are respectively $IS = 0.34$ mm/s and $QS = 0.66$ mm/s for the first component; $IS = 0.33$ mm/s, $QS = -0.12$ mm/s and $H_{\text{eff}} = 35.2$ T for the second component. According to the reference data [17] they are characteristic for iron(III) cations in two phases — ferrihydrite and α - FeOOH , respectively. Three different components can be resolved in the second spectrum (Fig. 4b). Two of them are sextet components having very close calculated values of $IS = 0.36$ – 0.37 mm/s and $QS = 0.03$ mm/s, but different $H_{\text{eff}} = 49.8$ and 46.9 T. These hyperfine parameters are typical of Fe^{3+} ions in octahedral coordination in La-perovskite structure.

However the values of the hyperfine magnetic field are lower in comparison to that for a bulk well crystallized material. The registered H_{eff} values are close to previously reported $H_{\text{eff}} = 48.9$ T for mechanically milled

LaFeO_3 [18]. The third spectra component is doublet with $IS = 0.34$ mm/s and $QS = 0.55$ mm/s, which can be also attributed to iron(III) cations in nanosized LaFeO_3 particles with superparamagnetic behavior [18]. Therefore, the obtained spectra components can be regarded as Fe^{3+} -ions in octahedral coordination in LaFeO_3 lattice, that belong to particles having different size. The Mössbauer study results are in very good agreement with those obtained with XRD.

3.3. IR spectroscopy

IR study in the middle and far regions of prepared materials gives qualitative characterization of the samples (Fig. 5). Bands at wave numbers less than 600 cm^{-1} are connected with metal–oxygen vibrations. Comparison of the samples' spectra under 600 cm^{-1} with the spectrum of the La_2O_3 pure substance directs to conclusion that almost all amount of La_2O_3 has reacted. The shift of the band at 388 cm^{-1} toward higher wave numbers (for La_2O_3) and the bands at $355/346$, $566/529$, and 600 cm^{-1} are assigned to formation of new phase(s). Bands at 855 cm^{-1} and the wide band in the region 1250 – 1750 cm^{-1} are characteristic of carbonates and hydrocarbonates adsorbed on the sample surface [19]. The complex bands around 1480 cm^{-1} allow affirming that the ratio between carbonates and hydrocarbonates varies. The carbonates predominate in the case of samples LaFeO_3 and LaCoO_3 . Bands at about 3412 and 1635 and 2900 cm^{-1} are characteristic for the presence of H-bound OH groups and physically adsorbed water molecules on the surface and hydrocarbons.

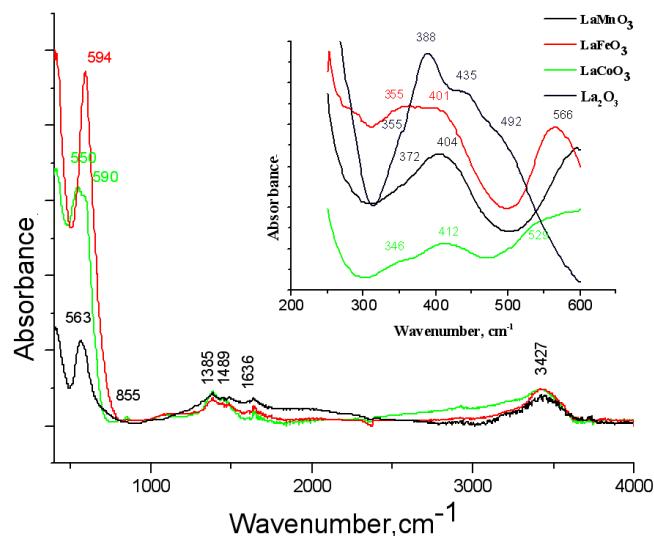


Fig. 5. IR spectra of synthesized perovskites in the middle region and in the far region (inset).

3.4. X-ray photoelectron spectroscopy

In order to determine the oxidation states and surface atomic concentration of the elements presented we

performed XPS study. The XP spectra of LaMO_3 ($M = \text{Fe, Mn, Co}$) are presented in Fig. 6. Figure 6a reveals that the spectrum of La consists of different oxidation type lanthanum for all three samples. The line

TABLE I

Surface atomic concentrations, at. %.

	La3d	Fe2p/Mn2p/Co2p	O1s
LaFeO_3	24	7	69
LaMnO_3	24	11	65
LaCoO_3	25	9	66

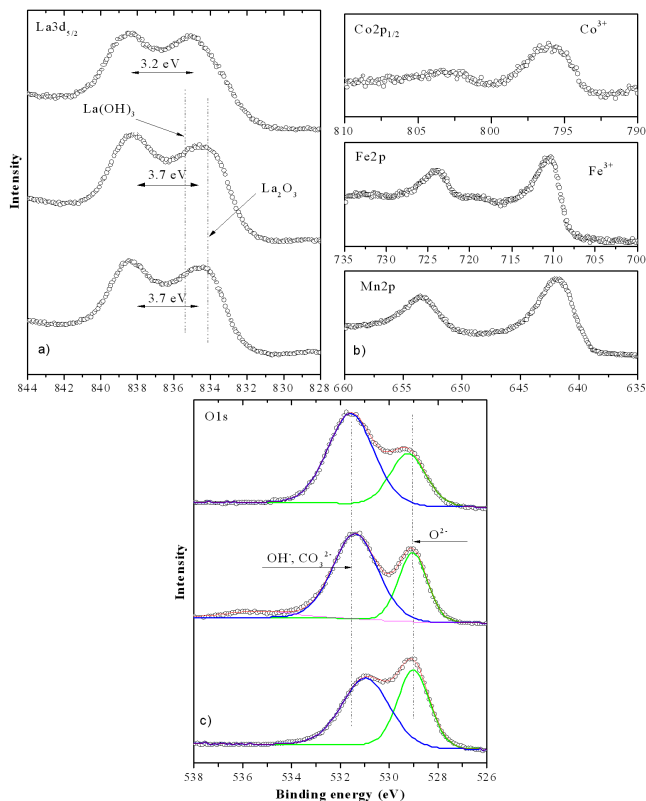


Fig. 6. XPS high-resolution spectra of LaMO_3 : (a) La 3d, (b) M 2p ($M = \text{Fe, Mn, Co}$) and (c) curve fitted O1s.

shape, binding energy (BE) and FWHM show that the peak can be curve fitted with two subpeaks with different ratio between them depending on sample. Using reference spectra these subpeaks can be ascribed as La^{3+} in La_2O_3 and $\text{La}(\text{OH})_3$ and/or $\text{La}_2(\text{CO}_3)_3$, which is in a very good agreement with IR analysis [20]. Surface atomic concentrations of all three samples LaMO_3 ($M = \text{Fe, Mn, Co}$) are given in Table. The estimated ratio between the elements differs from the theoretically expected 1:1:3. This discrepancy can be explained with the contamination of lanthanum carbonates and lanthanum hydroxides observed on the surface of the samples. Almost 2/3 (1/2) of measured lanthanum is connected with OH^- and/or CO_3^{2-} groups for LaFeO_3 and LaCoO_3 (LaMnO_3). In this way we can estimate ratio $\text{La:M} \approx 1:1$ ($M = \text{Fe, Mn, Co}$).

Figure 6b represents the Fe 2p peak. The registered BE and line shape together with the existence of shakeup satellite at ≈ 719 eV is typical for Fe^{3+} oxidation state. The measured BE of Mn 2p peak (Fig. 6b) is typical for Mn^{3+} oxidation state. Figure 6b shows Co 2p_{1/2} peak, too. The BE and line shape together with the existence of weak shakeup satellite at ≈ 800 –805 eV is typical for

Co^{3+} oxidation state.

The all three samples oxygen peak (Fig. 6c) can be fitted with two subpeaks, which are ascribed to OH^- and/or CO_3^{2-} groups with higher BE and O^{2-} with lower BE. The ratio between both subpeaks is close to 1:3, 1:1 and 1:2 for LaFeO_3 , LaMnO_3 and LaCoO_3 , respectively. Therefore, we can recalculate that the oxygen for all three samples is in the range of 25–35 at.%. Thus, the ratio $\text{La:M:O} \approx 1:1:3$ ($M = \text{Fe, Mn, Co}$), as expected for LaMO_3 ($M = \text{Fe, Mn, Co}$). As a conclusion we can say that the synthesized compounds are LaFeO_3 , LaMnO_3 , and LaCoO_3 . Because of the high chemical activity of the lanthanum element we have observed some impurity of La-carbonates and La-hydroxides on the surface of these samples, determined only by the surface sensitive XPS and IR techniques.

Synthesis of freshly synthesized compounds and their mechanoactivation can give rise to completely different results from those of MA of oxides. The phenomena of aggregation and agglomeration responsible for coarsening of size distribution during milling and mechanical activation are affected by the presence of water. Mechanical activation of hydroxides and oxyhydroxides lead to mechanically induced dehydroxylation and to formation of a porous substance with higher surface area and lower crystallite size [8]. Presented investigation shows a possibility to prepare perovskites with comparable characteristics (high dispersion, nanometric crystallite size about 10–20 nm, presence of oxygen vacancies) with previously reported studies [10–14] but using different synthesis procedure. The milling conditions are also comparable [10–14].

4. Conclusions

Perovskite-type LaMO_3 ($M = \text{Co, Fe, Mn}$) materials have been successfully prepared by a facile and environmentally friendly method starting from freshly precipitated Fe, Mn and Co oxides/hydroxides and their mechanical milling with lanthanum oxide. Single phase of LaMO_3 was obtained at room temperature, without any heating. In the case of Fe and Mn compounds the synthesis was done directly by milling of precursor and La_2O_3 but for Co-containing sample the single phase perovskite was synthesized after additional mechanoactivation of precipitated material. The spectroscopic data collected by XRD, Mössbauer spectroscopy, IR and XPS techniques reveal the properties of obtained materials. The prepared perovskites have nanometric crystallite size (about 15 nm), high dispersion, high degree of microstrains and high level of oxygen vacancies. Such charac-

teristics will be valuable for catalytic behavior of synthesized materials.

Acknowledgments

The financial support by the European Social Fund within the framework of Operating Program "Development of Human Resources" (BG051PO001-3.3.06-0050) for the preparation of this paper is gratefully acknowledged.

References

- [1] R. Köferstein, S. Ebbinghaus, *Solid State Ionics* **231**, 43 (2013).
- [2] N. Lakshminarayanan, J. Kuhn, S. Rykov, J.M. Millet, U. Ozkan, *Catal. Today* **157**, 446 (2010).
- [3] W. Zheng, R. Liu, D. Peng, G. Meng, *Mater. Lett.* **43**, 19 (2000).
- [4] X.P. Dai, Q. Wu, R.J. Li, C.C. Yu, Z.P. Hao, *J. Phys. Chem. B* **110**, 25856 (2006).
- [5] Z. Wei, Y. Xua, H. Liu, C. Hu, *J. Hazard. Mater.* **165**, 1056 (2009).
- [6] P. Dinka, A.S. Mukasyan, *J. Power Source* **167**, 472 (2007).
- [7] A. Giannakas, A. Ladavos, P. Pomonis, *Appl. Catal. B Environ.* **49**, 147 (2004).
- [8] P. Baláž, M. Achimovičová, M. Baláž, P. Billik, Z. Cherkezova-Zheleva, J.M. Criado, F. Delogu, E. Dutková, E. Gaffet, F.J. Gotor, R. Kumar, I. Mitov, T. Rojac, M. Senna, A. Streletskii, K. Wieczorek-Ciurowa, *Chem. Soc. Rev.* **42**, 7571 (2013).
- [9] K. Wieczorek-Ciurowa, K. Gamrat, *Mater. Sci.-Poland* **25**, 219 (2007).
- [10] S. Kaliaguine, A. Van Neste, V. Szabo, J.E. Gallot, M. Bassir, R. Muzychuk, *Appl. Catal. A Gen.* **209**, 345 (2001).
- [11] Q. Zhang, F. Saito, *J. Alloys Comp.* **297**, 99 (2000).
- [12] P. Ciambelli, V. Palma, S.F. Tikhov, V.A. Sadykov, L.A. Isupova, L. Lisi, *Catal. Today* **47**, 199 (1999).
- [13] T. Ito, Q. Zhang, F. Saito, *Powder Technol.* **143-144**, 170 (2004).
- [14] S. Ohara, H. Abe, K. Sato, A. Kondo, M. Naito, *J. Eur. Ceram. Soc.* **28**, 1815 (2008).
- [15] G.K. Williamson, W.H. Hall, *Acta Metall.* **1**, 22 (1953).
- [16] J.H. Scofield, *J. Electron Spectrosc. Relat. Phenom.* **8**, 129 (1976).
- [17] R.M. Cornell, U. Schwertmann, *The Iron Oxides*, Wiley-VCH, Weinheim 2003.
- [18] F.J. Berry, X. Ren, J.R. Gancedo, J.F. Marco, *Hyperfine Interact.* **156-157**, 335 (2004).
- [19] L.H. Little, *Infrared Spectra of Adsorbed Species*, Academic Press, London 1966, LCCCN: 65-27318.
- [20] G. Tyuliev, D. Panayotov, I. Avramova, D. Stoichev, Ts. Marinova, *Mater. Sci. Eng. C* **23**, 117 (2003).